Momentum dependent mean-fields of hyperons & antihyperons

Arsenia Chorozidou[1,*] and *Theodoros* Gaitanos[1,**]

[1]Department of Physics, Aristotle University of Thessaloniki

Abstract. The in-medium properties of hyperons and antihyperons are studied with the Non-Linear Derivative (NLD) model and focus is made on the momentum dependence of strangeness optical potentials. The NLD model is based on the Relativistic Mean Field (RMF) approximation to Relativistic Hadrodynamics (RHD) approach of nuclear systems, but it incorporates an explicit momentum dependence of mean-fields. The extension of the NLD model to the baryon and antibaryon octet is based on SU(6) and G-parity arguments. It is demonstrated that with a proper choice of momentum cut-offs, the Λ and Σ optical potentials are consistent with recent studies of the chiral effective field theory (χ -EFT) and optical potentials are consistent with Lattice-QCD calculations, over a wide momentum region. We also present NLD predictions for the in-medium momentum dependence of $\bar{\Lambda}$, $\bar{\Sigma}$ and $\bar{\Xi}$ hyperons. This work is important for future experimental studies, like CBM, PANDA at FAIR and is relevant to nuclear astrophysics as well.

1 Introduction

In an attempt to explain both astrophysical observations ($2M_\odot$ Neutron Stars, that seems to exclude soft hadronic Equation of State (EoS) at high baryon densities) and results from Heavy-Ion Collisions (they lead to a softening of the high-density EoS) with a proper nuclear matter model, an inclusion of hyperons degrees of freedom is performed in the NLD model. The NLD model is based on a basic RMF Lagrangian formulation, but it incorporates higher order derivatives in the nucleon-nucleon (NN) interaction Lagrangians. In previous work [1], it has been demonstrated that this Ansatz corrects the high-momentum behaviour of the interaction, makes the EoS softer at densities just above saturation, but at the same time it reproduces the $2M_\odot$ pulsars at densities far beyond saturation. Given that the NN interaction is fairly well known in contrast to the hyperon-nucleon (YN) interaction, in order to approach YN interaction, we take the tested for nucleons NLD model and extend it to the strangeness degrees of freedom, in the spirit of SU(6) and G-parity arguments. Having done that, we discuss the momentum dependence of the in-medium YN-potentials.

*e-mail: achoro@auth.gr
**e-mail: tgaitano@auth.gr

2 The NLD model for the baryon octet

The NLD Lagrangian is based on the conventional RHD and for the baryon octet it reads as

$$\begin{aligned}\mathcal{L} =& \frac{1}{2}\sum_B \left[\overline{\Psi}_B\gamma_\mu i\overrightarrow{\partial}^\mu\Psi_B - \overline{\Psi}_B i\overleftarrow{\partial}^\mu\gamma_\mu\Psi_B\right] \\ &- \sum_B m_B\overline{\Psi}_B\Psi_B - \frac{1}{2}m_\sigma^2\sigma^2 + \frac{1}{2}\partial_\mu\sigma\partial^\mu\sigma - U(\sigma) \\ &+\frac{1}{2}m_\omega^2\omega_\mu\omega^\mu - \frac{1}{4}F_{\mu\nu}F^{\mu\nu} \\ &+\frac{1}{2}m_\rho^2\vec{\rho}_\mu\vec{\rho}^\mu - \frac{1}{4}\vec{G}_{\mu\nu}\vec{G}^{\mu\nu} - \frac{1}{2}m_\delta^2\vec{\delta}^2 + \frac{1}{2}\partial_\mu\vec{\delta}\;\partial^\mu\vec{\delta} \\ &+\mathcal{L}_{int}^\sigma + \mathcal{L}_{int}^\omega + \mathcal{L}_{int}^\rho + \mathcal{L}_{int}^\delta\,. \end{aligned} \quad (1)$$

The sum over B runs over the baryonic octet

$$\Psi_B = (\Psi_N, \Psi_\Lambda, \Psi_\Sigma, \Psi_\Xi)^T \quad (2)$$

with

$$\Psi_N = (\psi_p, \psi_n)^T, \;\; \Psi_\Lambda = \psi_\Lambda \quad (3)$$

$$\Psi_\Sigma = (\psi_{\Sigma^+}, \psi_{\Sigma^0}, \psi_{\Sigma^-})^T, \;\; \Psi_\Xi = (\psi_{\Xi^0}, \psi_{\Xi^-})^T \quad (4)$$

for the isospin-doublets Ψ_N and Ψ_Ξ, isospin-triplet Ψ_Σ and the neutral Ψ_Λ. The interactions between the nucleon fields are described by the exchange of meson fields. These are the scalar σ and vector ω^μ mesons in the isoscalar channel, as well as the scalar $\vec{\delta}$ and vector $\vec{\rho}^{\,\mu}$ mesons in the isovector channel. Their corresponding Lagrangian densities are of the Klein-Gordon and Proca types, respectively Eq. (5, 6 and 7). The term $U(\sigma) = \frac{1}{3}b\sigma^3 + \frac{1}{4}c\sigma^4$ contains the usual selfinteractions of the σ meson. The notations for the masses of fields in Eq. (1) are obvious. The field strength tensors are defined as $F^{\mu\nu} = \partial^\mu\omega^\nu - \partial^\nu\omega^\mu$, $\vec{G}^{\,\mu\nu} = \partial^\mu\vec{\rho}^{\,\nu} - \partial^\nu\vec{\rho}^{\,\mu}$ for the isoscalar and isovector fields, respectively. In the following we restrict to a minimal set of interaction degrees of freedom. In the iso-scalar sector, the σ- and ω-fields are obviously considered. In the iso-vector channel, we keep the vector, isovector ρ-meson field and neglect the δ-field.

The NLD interaction Lagrangians contain the conventional and simple combinations between the bilinear baryon-and linear meson-fields, however, they are extended by the inclusion of non-linear derivative operators $\overrightarrow{\mathcal{D}}, \overleftarrow{\mathcal{D}}$ for each baryon species B:

$$\mathcal{L}^{\sigma}_{int} = \sum_B \frac{g_{\sigma B}}{2}\left[\overline{\Psi}_B\overleftarrow{\mathcal{D}}_B\Psi_B\sigma + \sigma\overline{\Psi}_B\overrightarrow{\mathcal{D}}_B\Psi_B\right] \quad (5)$$

$$\mathcal{L}^{\omega}_{int} = -\sum_B \frac{g_{\omega B}}{2}\left[\overline{\Psi}_B\overleftarrow{\mathcal{D}}_B\gamma^\mu\Psi_B\omega_\mu + \omega_\mu\overline{\Psi}_B\gamma^\mu\overrightarrow{\mathcal{D}}_B\Psi_B\right] \quad (6)$$

$$\mathcal{L}^{\rho}_{int} = -\sum_B \frac{g_{\omega\rho}}{2}\left[\overline{\Psi}_B\overleftarrow{\mathcal{D}}_B\gamma^\mu\vec{\tau}\Psi_B\vec{\rho}_\mu + \vec{\rho}_\mu\overline{\Psi}_B\vec{\tau}\gamma^\mu\overrightarrow{\mathcal{D}}_B\Psi_B\right] \quad (7)$$

for the isoscalar-scalar, isoscalar-vector and isovector-vector vertices, respectively. The arrows on the non-linear operator $\mathcal{D}$ indicate the direction of their action. The only difference with respect to the conventional RHD interaction Lagrangian is the presence of additional operator functions $\overrightarrow{\mathcal{D}}_B$, $\overleftarrow{\mathcal{D}}_B$. These operator functions will regulate the high momentum component of hyperons. These operator functions (or regulators) $\overrightarrow{\mathcal{D}}_B$, $\overleftarrow{\mathcal{D}}_B$ are hermitician and generic functions of partial derivative operator. That is, $\overrightarrow{\mathcal{D}}_B := \mathcal{D}\left(\overrightarrow{\xi}_B\right)$ and $\overleftarrow{\mathcal{D}}_B := \mathcal{D}\left(\overleftarrow{\xi}_B\right)$ with the operator arguments $\overrightarrow{\xi}_B = -\zeta^\alpha_B i\overrightarrow{\partial}_\alpha$, $\overleftarrow{\xi}_B = i\overleftarrow{\partial}_\alpha\zeta^\alpha_B$. The four vector $\zeta^\mu_B = v^\mu/\Lambda_B$ contains the cut-off Λ_B and v^μ is an auxiliary vector. They are assumed to act on the baryon spinors Ψ_B and $\overline{\Psi}_B$ by a formal Taylor expansion with respect to the operator argument. The functional form of the regulators is constructed such that in the limit $\Lambda_B \to \infty$ the original RHD Lagrangians are recovered, that is, $\overrightarrow{\mathcal{D}}_B = \overleftarrow{\mathcal{D}}^\dagger_B \to 1$.

From the generalised Euler-Lagrange formalism, we obtain the equations of motion for the degrees of freedom in the NLD model. The meson field equations of motion read

$$\partial_\alpha\partial^\alpha\sigma + m^2_\sigma\sigma + \frac{\partial U}{\partial\sigma} = = \frac{1}{2}\sum_B g_{\sigma B}\left[\overline{\Psi}_B\overleftarrow{\mathcal{D}}_B\Psi_B + \overline{\Psi}_B\overrightarrow{\mathcal{D}}_B\Psi_B\right], \quad (8)$$

$$\partial_\mu F^{\mu\nu} + m^2_\omega\omega^\nu = = \frac{1}{2}\sum_B g_{\omega B}\left[\overline{\Psi}_B\overleftarrow{\mathcal{D}}_B\gamma^\nu\Psi_B + \overline{\Psi}_B\gamma^\nu\overrightarrow{\mathcal{D}}_B\Psi_B\right], \quad (9)$$

$$\partial_\mu G^{\mu\nu} + m^2_\rho\vec{\rho}^{\,\nu} = = \frac{1}{2}\sum_B g_{\rho B}\left[\overline{\Psi}_B\overleftarrow{\mathcal{D}}_B\gamma^\nu\vec{\tau}\Psi_B + \overline{\Psi}_B\vec{\tau}\gamma^\nu\overrightarrow{\mathcal{D}}_B\Psi_B\right], \quad (10)$$

for the isoscalar-scalar, isoscalar-vector and isovector-vector exchange mesons, respectively. Each baryon-field obeys a Dirac-equation of the following type

$$\left[\gamma_\mu(i\partial^\mu - \Sigma^\mu_B) - (m_B - \Sigma_{sB})\right]\psi_B = 0\,, \quad (11)$$

with the selfenergies Σ^μ_B and Σ_{sB} defined as

$$\Sigma^\mu_B = g_{\omega_B}\omega^\mu\overrightarrow{\mathcal{D}}_B + g_{\rho B}\vec{\tau}_B\cdot\vec{\rho}^{\,\mu}\overrightarrow{\mathcal{D}}_B\,, \quad (12)$$

$$\Sigma_{sB} = g_{\sigma B}\sigma\overrightarrow{\mathcal{D}}_B\,. \quad (13)$$

Both Lorentz-components of the selfenergy, Σ^μ and Σ_s, show an explicit linear behavior with respect to the meson fields σ, ω^μ and $\vec{\rho}^{\,\mu}$ as in the standard RHD. However, they contain an additional dependence on the regulators. If we apply the RMF approximation to static hadronic matter (the spatial components of the meson fields in Minkowski- and isospin-spaces vanish, $\omega^\mu \to (\omega^0, \vec{0})$ and $\vec{\rho}^{\,\mu} \to (\rho^0_3, \vec{0}_3)$), we end up to the following forms

for the NLD meson-field equations

$$m_\sigma^2\sigma + \frac{\partial U}{\partial \sigma} = \sum_B g_{\sigma B} \left\langle \overline{\psi}_B \mathcal{D}_B \psi_B \right\rangle = \sum_B g_{\sigma B} \rho_{sB} \,, \tag{14}$$

$$m_\omega^2\omega = \sum_B g_{\omega B} \left\langle \overline{\Psi}_B \gamma^0 \mathcal{D}_B \Psi_B \right\rangle = \sum_B g_{\omega B} \rho_{0B} \tag{15}$$

with the scalar and vector density sources

$$\rho_{sB} = \int\limits_{|\vec{p}|\leq p_{F_B}} d^3p \, \frac{m_B^*}{\Pi_B^0} \, \mathcal{D}_B(p) \,, \tag{16}$$

$$\rho_{0B} = \int\limits_{|\vec{p}|\leq p_{F_B}} d^3p \, \frac{E_B^*}{\Pi_B^0} \, \mathcal{D}_B(p) \,. \tag{17}$$

The isovector densities are calculated through the standard isospin relations. For a hyperon with a given momentum relative to nuclear matter at rest (at a given nucleon density and isospin asymmetry) the mesonic sources contain only nucleons, $B = p, n$.

The meson-field equations of motion show a similar structure as those of the standard RMF approximation. However, the substantial difference between NLD and other conventional RMF models appears in the source terms which now contain in addition the momentum-dependent regulators $\mathcal{D}_B$. This is an important feature of the NLD model. The cut-off leads naturally to a particular suppression of the vector field at high densities or high Fermi-momenta in agreement with phenomenology, as discussed in detail in the previous work [1]. This feature is absent in conventional RHD approaches, except if one introduces by hand additional and complicated scalar/vector self-interactions.

The key observable for general discussions related to momentum or energy dependencies of in-medium hadronic potentials is the Schrödinger-equivalent optical potential U_{opt}, which is a complex quantity. The imaginary part describes the scattering processes of a given particle, e.g. a hyperon, with a nucleon of nuclear matter. The real part of the optical potential is related to the mean-field that a particle, e.g. a hyperon with a given momentum, experiences in the nuclear medium at a given density and isospin-asymmetry. The imaginary part of U_{opt} cannot be calculated within a conventional RMF prescription. However in the NLD model (given that it contains an explicit momentum dependence of the mean-fields and thus of the optical potential) we can give, at least, estimations for the imaginary part. We do this in the case of anti-hyperons. The real part of the Schrödinger-equivalent optical potential for hyperons is obtained from a non-relativistic reduction of the Dirac-equation and reads

$$U_{opt}^B = -S_B + \frac{E_B}{m_B} V_B + \frac{1}{2m_B} \left(S_B^2 - V_B^2 \right) . \tag{18}$$

It describes the in-medium interaction of a baryon species B with a momentum p, or single-particle energy $E_B = E_B(p)$, relative to nuclear matter at rest at a given density and isospin asymmetry. We will compare the NLD results with recent microscopic calculations from χ-EFT [2, 3] and Lattice-QCD [4] for the hyperon in-medium potentials.

3 Results

We consider nuclear matter at rest, at a given density, isospin asymmetry and at zero temperature, in which hyperons are situated at a given momentum relative to the nuclear matter at rest. The quantity of interest is the optical potential U_{opt} of the in-medium hyperons. There is no experimental information on the momentum dependence of the in-medium hyperonic potentials, so, as it has been mentioned before, we use for comparison some recent microscopic calculations. For Λ and Σ hyperons we compare with calculations based on the chiral-Effective Field Theory [2, 3] and for the Ξ hyperon we compare with calculations based on Lattice-QCD [4]. In the NLD calculations we take as a parameter only the strangeness cut-off of the hyperons and it has a monopole form

$$\mathcal{D}_Y(p) = \frac{{\Lambda_{\gamma_1}}^2}{{\Lambda_{\gamma_2}}^2 + \vec{p}^{\,2}} \,, \tag{19}$$

with $\gamma = \sigma, \omega, \rho$ indicating the cut-off values for the hyperon-nucleon σ, ω and ρ vertices, respectively, and $Y = \Lambda, \Sigma, \Xi$ denotes the hyperon type.

At first, the cut-offs of the hyperons have to be determined. The strangeness S=1 cut-offs are adjusted to the corresponding hyperonic optical potentials at saturation density of symmetric and cold nuclear matter from χ-EFT calculations. This is shown in Fig. 1 for the optical potential of Λ-hyperons and in in Fig. 2 for the optical potential of Σ-hyperons. The NLD calculations are able to describe the microscopic χ-EFT results in NLO very well. The corresponding values for the strangeness cut-off's are tabulated in Table 1.

Λ_σ	Λ_{ω_1}	Λ_{ω_2}	Λ_{ρ_1}	Λ_{ρ_2}
Λ cut-off				
0.7	0.85	0.79	–	–
Σ cut-off				
0.67	0.95	0.79	0.47	0.47
			0.63	0.5
Ξ cut-off				
0.6	0.8	0.71	1.3	1.2

Table 1. Λ-, Σ- and Ξ-regulators for σ- (Λ_σ), ω-($\Lambda_{\omega_{1,2}}$) & ρ-hyperon ($\Lambda_{\rho_{1,2}}$) vertices in units of GeV. In the cases for Σ and Ξ the isospin cut-offs ($\Lambda_{\rho_{1,2}}$) are relevant for the charged particles only. For the Σ-hyperon different cut-offs values are used for Σ^- (upper line) and for Σ^+ (bottom line).

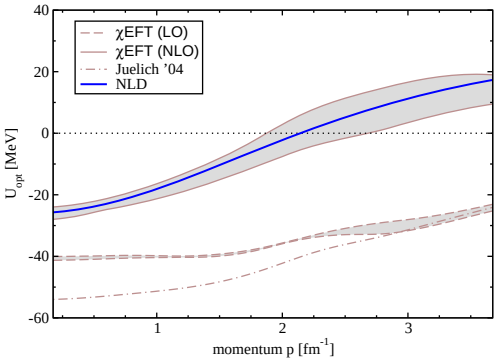

Figure 1. Optical potential of Λ-hyperons as function of their momentum p in symmetric nuclear matter at saturation density. The NLD-results (thick-solid curve) are compared with χ-EFT microscopic calculations at different orders LO (band with closed dashed borders) and NLO (band with closed solid borders). Further microscopic calculations of the Jülich group (dot-dashed curve) are shown too.

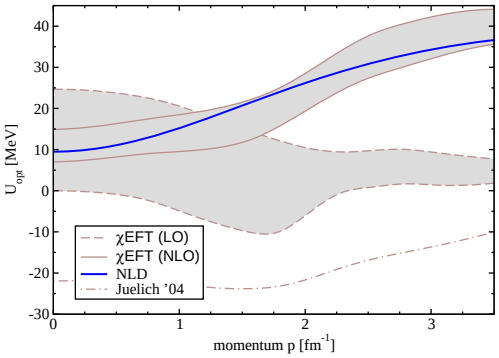

Figure 2. Same as in Fig. 1, but for Σ-hyperons.

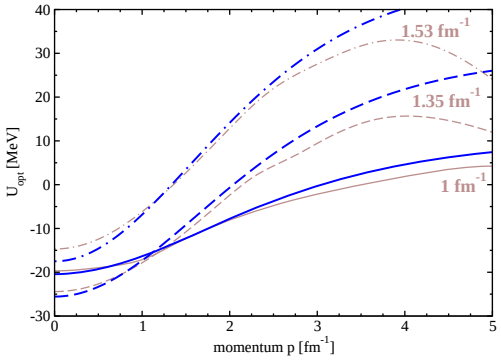

Figure 3. Optical potential of Λ-hyperons versus their momentum at various densities of symmetric nuclear matter. The NLD calculations at three Fermi-momenta (thick-solid, thick-dashed and thick-dot-dashed curves) as indicated are compared to the χ-EFT calculations in NLO.

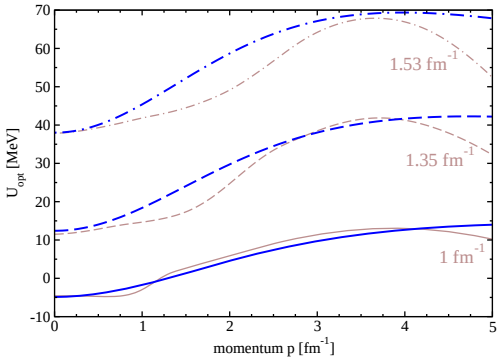

Figure 4. Same as in Fig. 3, but for the Σ-hyperons.

In Figs. 3 and 4 we show the predictive power of the NLD approach for Λ and Σ hyperons respectively, by comparing in more detail the density and momentum dependence of the NLD formalism with the χ-EFT calculations. We do this at various densities of symmetric nuclear matter.

In Figure 5 there are results for pure neutron matter at three different baryon densities. The NLD model does predict the general microscopic trends.

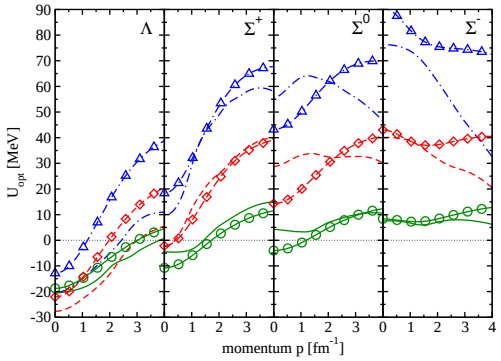

Figure 5. Optical potentials for hyperons (as indicated) versus their momentum for pure neutron matter. Solid curves with symbols indicate the NLD calculations while pure curves without symbols are the microscopic χ-EFT results from [2]. Green pairs (circles-solid for NLD and solid for χ-EFT) refer to low density of $p_F = 1$ fm^{-1}, red pairs (diamonds-solid for NLD and dashed for χ-EFT) refer to saturation density of $p_F = 1.35$ fm^{-1} and blue pairs (triangles-solid for NLD and dashed-dotted for χ-EFT) refer to a density of $p_F = 1.53$ fm^{-1}.

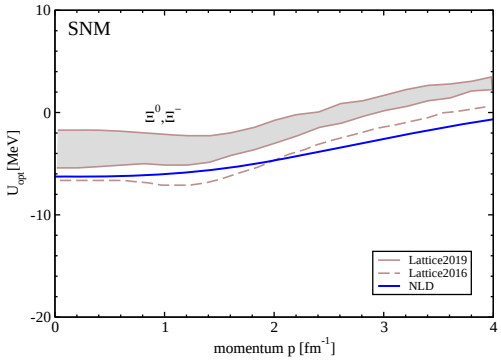

Figure 6. Optical potential of cascade hyperons versus their momentum for symmetric nuclear matter (SNM) at saturation density. The solid curve indicates the NLD predictions while the dashed curve and the gray band refer to recent Lattice calculations from Refs. [4].

Finally, in Figs. 6 and 7 we have the comparison of NLD model with recent microscopic calculations from Lattice-QCD for the cascade-hyperons, for both symmetric nuclear matter (SNM) and pure neutron matter (PNM).

In Figure 8 the predictions of NLD for anti-hyperon in-medium potentials are presented as well. The motivation for this study of anti-hyperons is the future experiments, such as those at FAIR, where the in-medium properties of anti-

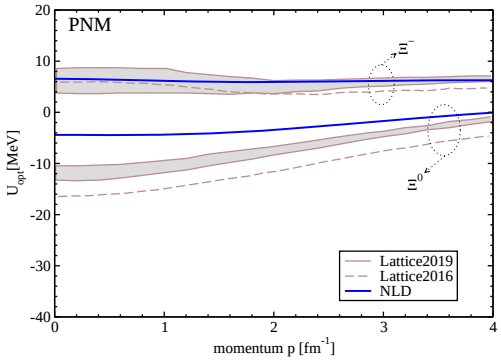

Figure 7. Same as in Fig. 6, but for pure neutron matter (PNM). The curves and bands belonging to Ξ^- and Ξ^0 are indicated in this figure.

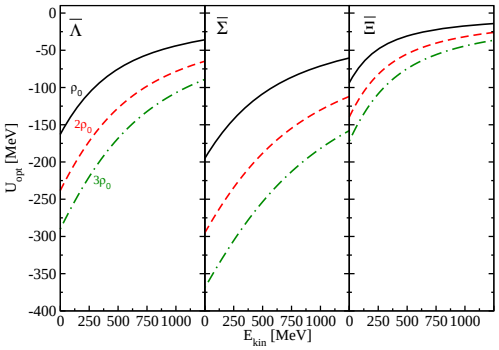

Figure 8. Optical potentials for anti-hyperons versus their kinetic energy for symmetric nuclear matter (SNM) at various densities, as indicated. The NLD predictions for saturation density ρ_0 (solid) and higher densities of $2\rho_0$ (dashed) and $3\rho_0$ (dashed-dot) are shown.

hadrons will be investigated too. In general for anti-particles the imaginary part of U_{opt} may be also important, so it is showed in the same figure as well. In the NLD approach the Im(U_{opt}) has been estimated from dispersion relations [1] and it is noticeable that it is comparable with its corresponding real part, particularly at very low energies. Possible physical explanations for that is that in antinucleon-nucleon scattering annihilation can occur through the production of light pions or the interaction of anti-hyperons with nucleons can happen via the production of the heavier kaons due to strangeness conservation (it may affect the Im(U_{opt}) at low energies).

References

[1] T. Gaitanos, M. Kaskulov, Nucl. Phys. **A 899**, 133 (2013) .
T. Gaitanos, M. Kaskulov, Nucl. Phys. **A 940**, 181 (2015).

[2] S. Petschauer et al. , Eur. Phys. J. **A 52**, 15 (2016).

[3] J. Haidenbauer, U.G. Meißner, A. Nogga, Eur. Phys. J. **A 56 (3)**, 91 (2020).

[4] T. Inoue, LATTICE-HAL QCD PoS INPC2016, 277 (2016).
T. Inoue, HAL QCD AIP Conf. Proc. 2130(1), 020002 (2019).